Intermodulation Analysis of the Collector-Up InGaAs/InAlAs/InP HBT Using Volterra Series

Bin Li and Sheila Prasad

***Abstract*— The intermodulation (IM) distortion of the collector-up InGaAs/InAlAs/InP heterojunction bipolar transistor (HBT) is analyzed using Volterra-series theory. A T-equivalent circuit is used for this analysis. The contribution and interaction of four nonlinear elements: base–emitter resistance, base–emitter capacitance, base–collector capacitance, and common base–current gain are analyzed. For the particular device under investigation, it is found that the cancellation effect is not significant and the base–emitter resistance nonlinearity dominates the third-order IM.**

***Index Terms*—Collector-up HBT, intermodulation, Volterra series.**

I. Introduction

Heterojunction bipolar transistors (HBT's) have been widely used in microwave power applications. Nonlinearity creates intermodulation (IM) distortion and is one of the key issues in power-application design. The Volterra series has been extensively used for modeling frequency-dependent distortion in weakly nonlinear circuits [1], [2] or for a small-signal excitation. Compared to harmonic-balance analysis, this technique provides the ability to understand the contribution and interaction of each nonlinear element. Much work has been done to explain the good linearity properties of HBT's despite the high exponential nonlinearity existing in the base–emitter junction. The partial cancellation effect of the IM currents generated by the base–emitter resistive and capacitive elements has been reported by Maas [3]. A cancellation effect through the interaction of the base–emitter nonlinear resistance and current gain has been reported by Samelis [4].

Since InGaAs-based HBT's are mainly used in low-power high-speed applications, not much work has been carried out on their power characteristics. A low third-order intercept point (IP3) (13 dBm) has been reported in [5] for the collector-up InGaAs/InAlAs/InP HBT's. This paper presents an IM analysis for collector-up HBT's based on the Volterra-series theory and explains why the low IP3 is present in InGaAs/InAlAs/InP HBT's. A T-equivalent circuit based on physical mechanisms is used. Section II gives the large-signal model and Volterra-series-analysis procedure. Section III gives the experimental characterization. Section IV analyzes the interaction of nonlinear elements and compares the measurement and simulation results. The conclusion is given in Section V.

II. Volterra-Series Analysis

The large-signal equivalent circuit of the collector-up HBT used for IM analysis is shown in Fig. 1. Since the extrinsic base–collector capacitance is negligible in the collector-up HBT's [6], [7], the equivalent circuit is simpler than that of the normal HBT. The technique used for extracting the element values is discussed in Section III. The four major sources of nonlinearity are: 1) the base–emitter resistance $g_{\rm be}$; 2) the base–emitter capacitance $c_{\rm be}$; 3) the base–collector capacitance $c_{\rm bc}$; and 4) the common base–current gain α. Under small-signal excitation, the base–emitter resistive characteristic can be expressed as a Taylor series in the vicinity of the bias point

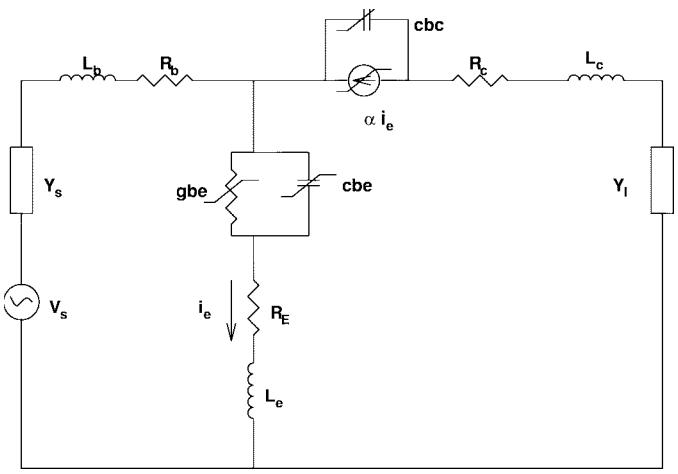

Fig. 1. The large-signal equivalent circuit of the collector-up HBT.

$$i_{gbe} = g_1 v_{\rm be} + g_2 v_{\rm be}^2 + g_3 v_{\rm be}^3 \tag{1}$$

where g_i, $i = 1, 2, 3$ are polynomial coefficients and $v_{\rm be}$ is the base–emitter small-signal voltage.

The base–emitter and base–collector capacitances have the small-signal charge/voltage characteristic

$$q_{\rm cbe} = c_1 v_{\rm be} + c_2 v_{\rm be}^2 + c_3 v_{\rm be}^3 \tag{2}$$

$$q_{\rm cbc} = c_1' v_{\rm bc} + c_2' v_{\rm bc}^2 + c_3' v_{\rm bc}^3 \tag{3}$$

where c_i and c_i', like g_i, are polynomial coefficients. The small-signal current in the capacitance is $\partial q_{\rm cbe}/\partial t$ and $\partial q_{\rm cbc}/\partial t$.

The nonlinearity of the common base–current gain is described as

$$\alpha = \alpha_{\rm dc} \frac{1}{1 + j\omega/\omega_\alpha} e^{-j\omega\tau} \tag{4}$$

$$\alpha_{\rm dc} = \alpha_1' + \alpha_2' i_e + \alpha_3' i_e^2. \tag{5}$$

For simplicity, the bias dependence and the frequency dependence of α are considered to be uncorrelated. In fact, the transit time τ and ω_α are both functions of dc bias. The error introduced by the assumption should not be significant since the frequency used for IM analysis has not gone up to the millimeter frequency level and a lower power input is used in the measurement and analysis (the bias swing would be small). Moreover, the transit time is insensitive to the bias variation because there is an undoped buffer layer between base and collector [8]. For large power inputs and millimeter-wave applications where the transit time effects and voltage swings are much larger, the above assumption has to be reexamined for small errors [9].

Therefore, after rearrangement we have

$$\alpha = \alpha_1 + \alpha_2 i_e + \alpha_3 i_e^2 \tag{6}$$

where $\alpha_i = \alpha_i'[1/(1 + j\omega/\omega_\alpha)] \times e^{-j\omega\tau}$, $i = 1, 2, 3$.

The nonlinear-current method [10] was used to implement the Volterra-series theory. In this technique, current components are calculated from voltage components of lower order. Voltage components of the same order are then determined from those currents, and the

Manuscript received September 2, 1997; revised May 4, 1998. This research was supported in part by the National Science Foundation under Grant ECS-9529643.

The authors are with the Department of Electrical and Computer Engineering, Northeastern University, Boston, MA 02115 USA.

Publisher Item Identifier S 0018-9480(98)06161-4.

TABLE I
THE PARAMETER VALUES FOR VOLTERRA-SERIES ANALYSIS

Parameters	Values
$R_b\ (\Omega)$	170
$R_c\ (\Omega)$	19
$R_E\ (\Omega)$	42.8
L_c (pH)	140
L_b (pH)	16
L_e (pH)	10
α_1'	0.96
α_2'	0.8
α_3'	0
τ	1e-12
I_B (A)	0.17e-3
V_{BE} (V)	0.89
V_{BC} (V)	-0.61
I_C (A)	1.995e-3
$g_1\ (S)$	0.0713
$g_2\ (S/V)$	1.3017
$g_3\ (S/V^2)$	15.8339
$c_1\ (F)$	3.9686e-13
$c_2\ (F/V)$	3.9553e-12
$c_3\ (F/V^2)$	4.7529e-11
$c_1'\ (F)$	2.88e-14
$c_2'\ (F/V)$	2.81e-15
$c_3'\ (F/V^2)$	5.4934

next higher order currents are found. Therefore, nonlinear high-order load voltages and the power absorbed by the load can be easily evaluated.

III. EXPERIMENTAL CHARCACTERIZATION

The device under investigation is a $5 \times 10\ \mu\text{m}^2$ InGaAs/InAlAs/InP collector-up HBT with $f_T = 23$ GHz and $f_{\max} = 20$ GHz. The two-tone IM measurement at frequencies $f_1 = 6.02$ GHz and $f_2 = 6.08$ GHz was performed to verify the analysis. The magnitudes of two-tone signals are the same. The device was biased at the constant base–current with $I_B = 170\ \mu$A and $V_{\rm CE} = 1.5$ V. Multibias S-parameter measurements in the 0.45- to 40-GHz frequency range were performed using the HP8510 network analyzer and the Cascade probe station. Equivalent-circuit elements at each bias were extracted by fitting the equivalent-circuit parameters to minimize the error between simulated S-parameters and measured S-parameters. Parasitic and extrinsic elements L_c, L_b, L_e, R_b, R_c, and R_E are considered to be bias-independent, while four nonlinear elements are bias-dependent. The nonlinear elements are approximately assumed to be the function of only a single variable ($v_{\rm be}$, $v_{\rm bc}$, or i_e). This assumption greatly reduces the complexity of this analysis. The nonlinear base–emitter resistance was chosen as a representative example for illustrating the derivation of the polynomial coefficients in (1). The extracted small-signal conductance was fitted to a polynomial expression $g(V)$, where V represents the intrinsic base–emitter voltage. It is noted that $g(V) = (dI/dV)$, where $I(V)$ is the large-signal I–V characteristic to model the base–emitter resistance. Therefore,

$$g_1 = g(V_{\rm BE})$$
$$g_2 = 1/2\left.\frac{dg}{dV}\right|_{V=V_{\rm BE}}$$
$$g_3 = 1/6\left.\frac{d^2g}{dV^2}\right|_{V=V_{\rm BE}}. \tag{7}$$

Similar derivations are applied to the nonlinear elements $c_{\rm be}$, $c_{\rm bc}$, and α. All the values needed to perform a Volterra-series analysis are listed in Table I.

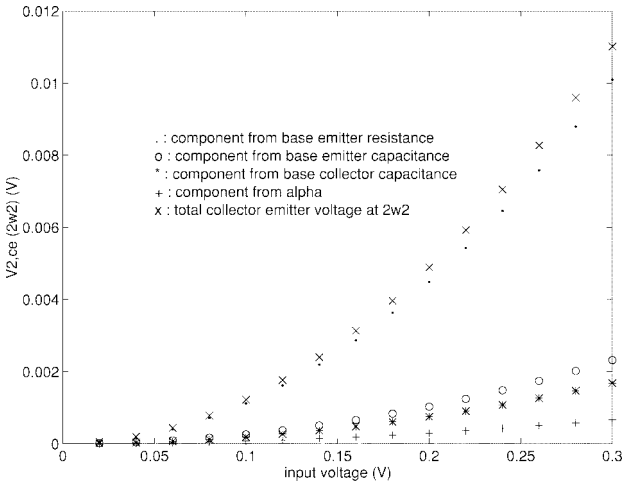

Fig. 2. $V_{2,\,\rm ce}(2\omega_2)$ versus the excitation voltage.

The source and load impedances are assumed to be 50 Ω at dc and at all mixing frequencies up to the third order. The measured terminations are very close to 50 Ω at dc and at mixing frequencies up to the third order. The selected bias point is $I_b = 170\mu$A, $V_{\rm ce} = 1.5$ V. There is no obvious difference if the measured impedances are used in this analysis.

IV. IM ANALYSIS

The calculation for voltage or current components at different mixing frequencies is straightforward from basic circuit theory once all the element values and polynomial coefficients are known. Fig. 2 shows the magnitudes of the collector–emitter voltage components at the frequency $2\omega_2$ versus the input voltage. The magnitude of the component from $g_{\rm be}$ is much larger than that from the other nonlinear elements. The phase differences of those components are considered constants if terminations are assumed to be 50 Ω at dc and at all mixing frequencies up to the third order. The phases of components from $g_{\rm be}$, $c_{\rm be}$, $c_{\rm bc}$, α are 0.11π, 0.61π, and -0.34π, and 0.23π, respectively. The phase difference between the components from $c_{\rm be}$ and $c_{\rm bc}$ is almost π and cancellation occurs between the components from these two elements. The phases of the components from $g_{\rm be}$ and α are almost identical; therefore, an enhancement effect occurs and the total voltage is a little larger than that from $g_{\rm be}$. Since the magnitudes of components from the capacitances are close to each other and the magnitude of α is much smaller, the final phase and magnitude of $V_{2,\,\rm ce}(2\omega_2)$ is dominated by the component from $g_{\rm be}$.

The collector–emitter voltage $V_{\rm ce}$ at frequency $\omega_1 - \omega_2$ is also dominated by the nonlinearity of the base–emitter resistance because the magnitude of components from $c_{\rm be}$, $c_{\rm bc}$, and α is very small, as shown in Fig. 3. The phases of components from $g_{\rm be}$, $c_{\rm be}$, $c_{\rm bc}$, and α are approximated to π, -0.50π, 0.50π, and π, respectively. The phase difference between $c_{\rm bc}$, $c_{\rm be}$ is π and cancellation should occur. The phases of components from $g_{\rm be}$ and α are the same, so some enhancement effect occurs. However, the significant difference between the magnitude of $V_{2,\,\rm ce}(\omega_2 - \omega_1)$ components generated by $g_{\rm be}$ and the other nonlinear elements make the cancellation and enhancement effects negligible. The second-order component at $\omega_2 - \omega_1$ is much larger than that at $2\omega_2$. Therefore, the voltage component at $2\omega_2 - \omega_1$ is dominated by the mixing product from the frequency $\omega_2 - \omega_1$ in this device. The contribution and impact of the nonlinear elements on IMD3 can be determined by examining the third-order nonlinear voltage $V_{\rm ce}$ generated by each element at frequency $2\omega_2 - \omega_1$. Fig. 4 shows the third-order nonlinear collector–emitter voltage generated by four nonlinear elements with

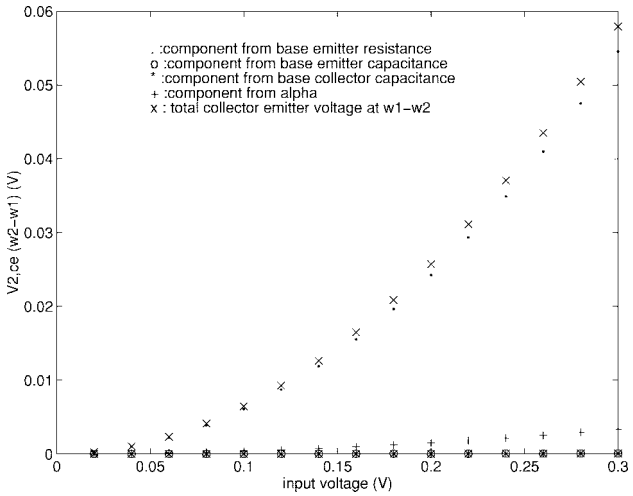

Fig. 3. $V_{2,\mathrm{ce}}(\omega_2 - \omega_1)$ versus the excitation voltage.

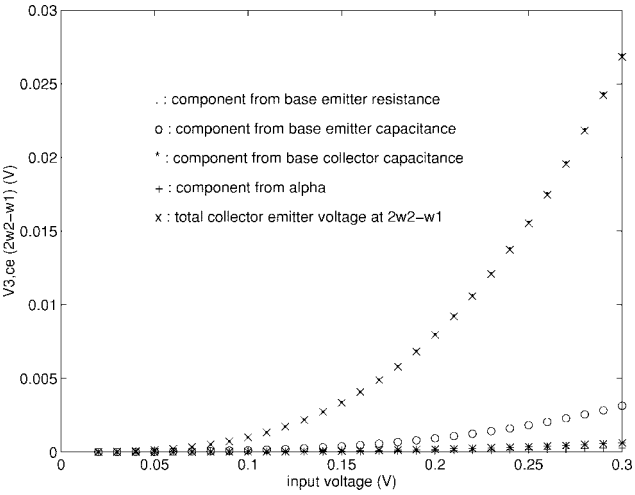

Fig. 4. The nonlinear voltage at $2\omega_2 - \omega_1$ generated by four nonlinear elements.

respect to the excitation voltage. In this particular device, at this bias point, it is observed that the magnitudes of $V_{3,\mathrm{ce}}(2\omega_2 - \omega_1)$ generated by c_{be}, c_{bc}, and α are much less than that generated by g_{be}. The phases of $V_{3,\mathrm{ce}}(2\omega_2 - \omega_1)$ generated from g_{be}, c_{be}, c_{bc}, and α are -0.66π, -0.16π, -0.18π, and 0.37π, respectively. The phase difference of nonlinear voltages from α and g_{be} is close to π, which confirms the possible cancellation effect reported by Samelis [4]. However, the magnitude of the nonlinear current from α is much smaller compared to that from g_{be}. Therefore, the components from α can be negligible and the cancellation is not significant. The phase difference of $V_{3,\mathrm{ce}}(2\omega_2 - \omega_1)$ generated from g_{be} and c_{be} is $\pi/2$. The same phase difference exists between the components of g_{be} and c_{bc}. Therefore, for this particular device, the nonlinearity of the base–emitter resistance dominates the third-order IM distortion (IMD3). The cancellation is hardly observed in the interaction of nonlinear elements. This also explains why the IMD3 (13 dBm) is so low in this particular device. The simulation and measurement results of the IMD3 are shown in Fig. 5.

V. Conclusions

The IM-distortion performance was studied by Volterra-series theory. The T-type equivalent circuit was used in this investigation. The polynomial coefficients of nonlinear elements are obtained by fitting nonlinear elements with respect to the bias variation. The nonlinear-current method was used to implement the Volterra-series theory. The results of this analysis show that the interactions and contributions of nonlinear elements are very much device dependent. For the device under study, the cancellation did occur. However, this cancellation was not significant due to the difference in magnitudes of the mixing components from the different nonlinear elements. The nonlinearity of this device is dominated by the base–emitter resistive nonlinearity. This also explains the low IM intercept point of this particular HBT.

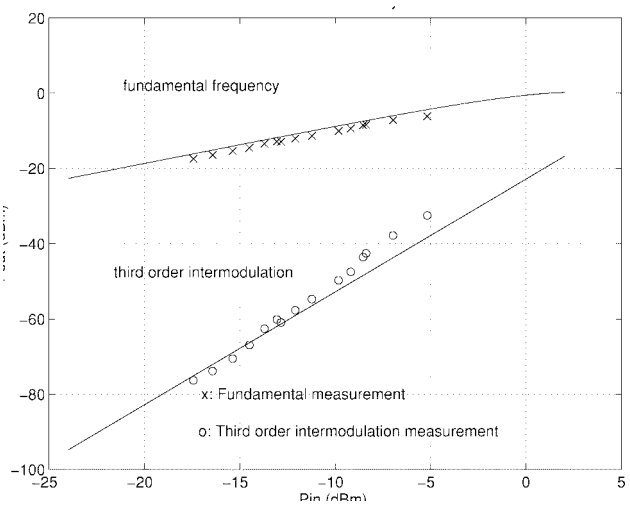

Fig. 5. The simulated and measured IMD3.

Acknowledgment

The authors wish to thank Dr. B. Meskoob for providing his measurement data. They also wish to thank Prof. C. G. Fonstad, Massachusetts Institute of Technology, Cambridge, for providing the devices and the use of laboratory facilities for this work.

References

[1] S. Narayanan, "Transistor distortion analysis using Volterra series representation," *Bell Syst. Tech J.*, vol. 46, p. 991, May/June 1967.

[2] G. M. Lambrianou and C. S. Aitchison, "Optimization of third order intermodulation product and output from X-band MESFET amplifier using Volterra series analysis," *IEEE Trans. Microwave Theory Tech.*, vol. MTT-33, pp. 1395–1403, Dec. 1985.

[3] S. A. Maas, B. L. Nelson, and D. L. Tait, "Intermodulation in heterojunction bipolar transistors," *IEEE Trans. Microwave Theory Tech.*, vol. 40, pp. 442–447, Mar. 1992.

[4] A. Samelis and D. Pavlidis, "Mechanism determining third order intermodulation distortion in AlGaAs/GaAs heterojunction bipolar transistors," *IEEE Trans. Microwave Theory Tech.*, vol. 40, pp. 2374–2380, Dec. 1992.

[5] B. Li and S. Prasad, "Harmonic and two-tone intermodulation distortion analyses of the inverted InGaAs/InAlAs/InP HBT," *IEEE Trans. Microwave Theory Tech.*, vol. 45, pp. 1135–1137, July 1997.

[6] B. Meskoob, S. Prasad, M. Vai, J. Vlcek, H. Sato, C. G. Fonstad, and C. Bulutay, "A small-signal equivalent circuit for the collector-up InGaAs/InAlAs/InP heterojunction bipolar transistor," *IEEE Trans. Electron Devices*, vol. 39, pp. 2629–2632, Nov. 1992.

[7] B. Meskoob, S. Prasad, M. Vai, J. C. Vlcek, H. Sato, and C. G. Fonstad, "Bias-dependence of the intrinsic element values of InGaAs/InAlAs/InP inverted heterojunction bipolar transistor," *IEEE Trans. Microwave Theory Tech.*, vol. 40, pp. 1012–1014, May 1992.

[8] W. Lee, "The fabrication and characterization of InGaAs/InAlAs/InP heterojunction bipolar transistors," Ph.D. dissertation, EECS Dept., MIT, Cambridge, MA, 1988.

[9] D. A. Teeter, J. R. East, R. K. Mains, and G. I. Haddad, "Large-signal numerical and analytical HBT models," *IEEE Trans. Electron Devices*, vol. 40, pp. 837–845, May 1993.

[10] S. A. Maas, *Nonlinear Microwave Circuits.* Piscataway, NJ: IEEE Press, 1997.